Eccentricity-Dependent Saccadic Reaction Time: The Roles of Foveal Magnification and Attentional Orienting

Yufeng Zhang[1, 2, 3, *], Pascal Fries[1, 2, 3]

[1]Ernst Strüngmann Institute (ESI) for Neuroscience in Cooperation with Max Planck Society, 60528 Frankfurt, Germany
[2]Donders Institute for Brain, Cognition and Behaviour, Radboud University, 6525 EN Nijmegen, the Netherlands
[3]International Max Planck Research School for Neural Circuits, 60438 Frankfurt, Germany
[*]Correspondence: yufeng.zhang@esi-frankfurt.de

Summary

A hallmark of primate vision is the emphasis on foveal processing, accompanied by frequent saccades that bring the fovea to salient parts of the scene, or to newly appearing stimuli. A saccade to a new stimulus is one of the most fundamental sensory-motor transformations. In macaque monkeys, we show that foveal magnification is not only the reason for saccades, but it also governs the dynamics of saccade initiation. In a task where the monkeys made saccades to peripheral target onsets, saccadic reaction time (SRT) increased with target eccentricity. Notably, we effectively eliminated this increment by scaling the target size according to the foveal magnification factor in the superior colliculus (SC). We repeated the comparison between non-scaled and scaled targets, while changing the task to a delayed saccade task. In this task, the target was presented long before the saccade, and the saccade was triggered by fixation offset rather than target onset, such that target onset was essentially irrelevant for SRT. Crucially, in this task, we found that SRT increased with target eccentricity, for both non-scaled and scaled targets. Furthermore, this increment survived the addition of a salient foveal distracting flash. The results obtained with the delayed saccades task are consistent with an attentional scan from the fovea to the target, a recently hypothesized general mechanism of attention.

Keywords

Eye movement; cortical magnification factor; superior colliculus; attentional orienting

Introduction

We make several saccades per second, redirecting our gaze to bring objects of interest into our high-resolution fovea. However, the time it takes to initiate a saccadic eye movement can vary significantly, even when the task is simple and highly repetitive. Part of the variability comes from the size of the impending saccade. Previous studies have shown that small saccades towards targets at an eccentricity below one degree of visual angle (dva) generally take longer to initiate across a wide range of experimental conditions [1, 2]. However, the relationship between saccadic reaction time (SRT) and target eccentricity for medium-sized saccades remains unclear [1, 2]. Yet, these medium-sized saccades between 2 and 10 dva constitute the most commonly executed saccades in daily life [3] and in laboratory settings, where SRTs are widely used as a tool to characterize the cognitive process of interest [4-6].

Previous studies describing the relationships between SRT and saccade size often utilized a *Step* task. In the *Step* task, the fixation dot moves into the periphery and becomes the saccade target. This design often comes with a significant confounding factor: saccade targets that are physically identical, vary in saliency across eccentricity and corresponding saccade size. This is because a visual stimulus of a given physical size undergoes foveal magnification early in the visual processing hierarchy [7-9] and therefore has decreasing salience for increasing eccentricity, or saccade size, respectively [10]. In addition to foveal magnification, low background lighting commonly employed in previous studies might have resulted in the target signal being very strong, such that the SRT showed a floor effect, which might have masked the effect of target eccentricity [11]. It is therefore important to control the strength of the afferent signal at different eccentricities in order to draw conclusions about the dependence of SRT on target eccentricity *per se*.

Besides physical stimulation, the nature of the impending saccade, as determined by the task structure, can also influence the relationship between SRT and target eccentricity. Hafed and Goffart [1] reported a clear effect of increasing SRT with target eccentricity in a visually guided saccade task. Despite the confounding factors mentioned earlier, when the same stimulus set was used for a *delayed* visually guided saccade task, the observed increase of SRT with eccentricity became minimal. This is interesting because the main difference between these two tasks is that in the visually guided saccade task, the response saccade is exogenously driven, dominated by the transient onset of the target stimulus; in contrast, in the *delayed* visually guided saccade, the response saccade is endogenously driven, triggered by fixation dot offset, far away from the target stimulus. The observation that the SRT in these two tasks exhibited different patterns of eccentricity dependence motivated us to look into these two types of saccades (endogenous saccades and exogenous saccades) separately.

Given exactly the same physical conditions and task structure, SRTs across trials can still exhibit high variability [12, 13]. The participant can very commonly make a response saccade as fast as 150 ms in one trial and as slow as 300 ms in another, physically identical, trial. Such high variability requires many trials to reveal a genuine but modest shift of the characteristic SRT. For example, more than 200 trials per condition are needed to reveal a shift of 10 ms for a typical SRT distribution (exponential modified Gaussian with peak at 200 ms and a standard deviation of 38 ms, two sided Mann-Whitney U test). Such trial counts were not obtained in previous studies.

The current study aims at addressing the aforementioned issues in macaque monkeys. We selected two sets of stimuli as saccade targets located between 2 and 10 dva (Figure 1A). One

set was *Equal*, having the same physical size at different eccentricities. The second set was *Scaled* based on the foveal magnification in the superior colliculus, aiming to equalize their input strength across eccentricities [8]. Note that even though we scaled the stimulus size according to the magnification factor in the SC, it has been suggested that this magnification factor is approximately shared between SC and the primary visual cortex [8]. To avoid dark adaptation, in all tasks, we presented the target on a gray background. We used the same stimuli sets in both, a *Step* (visually guided saccade) task and an *Overlap* (delayed visually guided saccade) task (Figure 1B-C). Additionally, in the *Overlap* task, we incorporated an extra condition including a transient attention-capturing distractor flash to investigate whether eccentricity-dependent attentional orienting is consistent with the eccentricity-dependent SRT changes for endogenous saccades. Last but not least, for each monkey and each condition, we collected more than 200 trials per condition to gain the necessary statistical power.

Results

Foveal magnification explains eccentricity dependent SRT increase for exogenously driven saccades

We started with exogenously driven saccades in the *Step* task (Figure 1B). The hypothesis is that the reported increase of SRT for exogenously driven saccades [1] is due to foveal magnification. To test this hypothesis, we designed two stimulus sets as saccade targets. The first set, *Equal*, was similar to what has been used in previous studies (Figure 1A, top). In this set, saccade targets at all positions were white filled circles of radius 0.1 dva. The second set, *Scaled*, consisted of filled white circles whose sizes were scaled according to the reported magnification factor in the SC, ensuring that they had the same spread, i.e. the same spatial extent of neuronal representation, in the SC (Figure 1A, bottom). Both sets consisted of stimuli positioned at 2, 3, 4, 5, 6, 8, and 10 dva to the right of the fixation point along the horizontal median. To facilitate comparison, the target stimulus at 2 dva was of the same size in the two sets.

Figure 1B illustrates the task structure for the *Step* task. In this task, each trial started with the monkey maintaining fixation on a fixation dot (0.1 dva filled white circle) for 800 to 1500 ms. Subsequently, the fixation dot was turned off. At the same video frame, a single saccade target randomly chosen from the combined *Equal* and *Scaled* stimuli set was presented. The monkey needed to make a saccade within 500 ms towards the target and hold its gaze on the target for another 800 to 1500 ms. If it completed the trial correctly, a juice reward was provided. Only correct trials were included in our analysis.

We first plotted the resulting SRT distributions for each condition (Figure 2A). The raw data revealed that: 1) Both location and shape of the SRT distribution varied across conditions and monkeys. 2) Similar to what has been reported before, the peak of the SRT distributions for *Equal* targets (blue) gradually increased with increasing target eccentricity. 3) This shift was significantly reduced for *Scaled* targets (orange) for all monkeys except monkey HU. 4) SRTs also became more variable as they became longer. We next quantified these observed patterns.

To quantify the effect of target eccentricity, we fitted a robust linear model ($SRT \sim \beta_0 + \beta_1 * (targetEccentricity - 2)$) separately for *Equal* and *Scaled* targets for each monkey (Figure 2B). For all monkeys, SRT increased with target eccentricity for both *Equal* and *Scaled* targets (positive β_1, α=.05, Bonferroni corrected for multiple comparisons across monkeys and

conditions). To test whether the slope in *Equal* and *Scaled* conditions were different, we next combined the data from the *Equal* and *Scaled* conditions and fitted a robust linear regression model that included an interaction term ($SRT \sim \beta_0 + \beta_1 * (targetEccentricity - 2) + \beta_2 * (targetEccentricity - 2) * IsScaled$). It turned out that for all monkeys except monkey HU, scaling decreased the slope (negative β_2, α=.05, Bonferroni corrected for multiple comparison across monkeys). For monkey HU, scaling increased the slope instead. Further analysis showed that the increased slope for the *Scaled* condition in monkey HU was produced by trials where the target was presented at 8 or 10 dva. When we limited our analysis to target eccentricities of 6 dva or less, the slope difference became insignificant for HU, while at the same time, scaling still decreased the slope significantly for the other monkeys. Because stimulus scaling had a different effect on HU than the other monkeys, suggesting that HU might have used a different strategy, we excluded HU in the following pooled analysis across monkeys (see Discussion, *Individual differences*).

For the analysis pooled over monkeys, we used a different approach. Note that in the previous analysis, even though we used robust linear regression to minimize the effect of heavy-tailedness in the SRT distribution, these tails were not outliers but features of SRT distribution [5, 12]. Additionally, distributions for targets at more periphery locations had larger variance which potentially biased our results. To address these limitations, we first fitted an exponentially modified Gaussian (exGauss, Figure 2A) for each SRT distribution. From each exGauss fit, we then extracted the mode to represent the typical value, and the full width at half maximum (FWHM) to represent the variability of the SRT distribution in that particular condition. To further facilitate combining data from different monkeys, we normalized the exGauss mode and FWHM such that for each monkey the normalized values spanned zero to one ($X_{normalized} = (X - X_{min})/(X_{max} - X_{min}$). These normalized values were then used for weighted linear regression analysis (Figure 2C, D, $Mode \sim \beta_0 + \beta_1 * targetEccentricity$ or $FWHM = \beta_0 + \beta_1 * targetEccentricity$). Importantly, for each data point, the inverse of the bootstrap variance was used as the weighting factor to further account for the variability in the shape of SRT distributions. The results supported our hypothesis: The mode of the SRT distribution increased with target eccentricity for *Equal* targets (Figure 2C, Blue; $CI_{\beta_1,95\%} = [.080,\ .136]$), but not for *Scaled* targets (Figure 2C, Orange;$CI_{\beta_1,95\%} = [-.022,\ .015]$). We separately fitted a model combining data from *Scaled* and *Equal* targets with the interaction term included ($Mode \sim \beta_0 + \beta_1 * (targetEccentricity - 2) + \beta_2 * (targetEccentricity - 2) * IsScaled$). The result showed that indeed "Scaling" reduced the slope ($CI_{\beta_2,95\%} = [-.134,\ -.091]$). We did the same analysis for FWHM (Figure 2D). The FWHM of the SRT distributions increased with target eccentricity for both, the *Equal* targets ($CI_{\beta_1,95\%} = [.088,\ .134]$) and the *Scaled* targets ($CI_{\beta_1,95\%} = [.033,\ .065]$), and scaling reduced the slope as shown by a significant interaction between these conditions ($CI_{\beta_2,95\%} = [-.085, -.050]$).

Foveal magnification modulated SRT in a similar fashion at different contrast levels but was most effective for low-contrast stimuli

The results in the previous section suggested that the observed SRT increment with increasing target eccentricity could be explained by foveal magnification. The potential mechanism could be that a stimulus closer to the fovea would activate a larger neuronal population in, for example, the SC. Then due to the lateral interaction pattern, neurons in this larger population would facilitate each other and result in a faster saccade initiation. Also a stimulus with higher contrast is known

to evoke a stronger and faster response throughout the visual hierarchy leading also to faster reaction times [14-17]. We next investigated how these two mechanisms interact.

To this end, we slightly modified the *Step* task that we had used so far. Firstly, we reduced the screen background luminance to allow for target contrast manipulation. Secondly, at each target location, for each target size, we selected three target luminance levels such that the resulting contrasts were evenly spaced on a logarithmic scale. Lastly, we limited target locations to 2, 4, and 6 dva to ensure an adequate number of trials for each condition. We collected data from one monkey (HO) for this modified *Step* task.

The resulting SRTs are plotted in Figure 3A. The pattern is similar to what has been described in the previous section. For *Equal* targets across all contrast levels, SRTs tended to be longer for more eccentric targets. Scaling, as described before, reduced this increment. Note that the effect of scaling, in terms of reducing the eccentricity-related SRTs increment, appeared to decrease with increasing contrast (Figure 3C). As before, we next quantified the observed effects with linear regression.

We first confirmed that increasing contrast, as expected, shortened SRTs. To quantify how target contrast affected SRTs for *Scaled* and *Equal* targets, we fitted an interaction model separately for each target location (Figure 3B, $SRT \sim \beta_0 + \beta_1 * logContrast + \beta_2 * isScaled + \beta_3 * logContrast * IsScaled$). The interaction term was significant for targets at 4 and 6 dva (H_0: β_3=0, α=.05, Bonferroni corrected for multiple comparisons across target positions). Because the target at 2 dva was physically identical in both stimulus sets, the interaction term was, as expected, insignificant. We next checked the simple effect of target contrast with a reduced model ($SRT \sim \beta_0 + \beta_1 * logContrast$) at each eccentricity for *Scaled* and *Equal* targets separately. It turned out that in all fits, except for the *Scaled* targets at 6 dva, increasing target contrast significantly shortened SRTs (H_0: β_1=0, α=0.05, Bonferroni corrected for multiple comparisons across target position and scaling groups). We then examined how target eccentricity affected SRT in the *Scaled* and *Equal* groups. Similar to the analysis of target contrast, we first fitted an interaction model separately for each target contrast level (Figure 3C, $SRT \sim \beta_0 + \beta_1 * (targetEccentricity - 2) + \beta_3 * (targetEccentricity - 2) * IsScaled$). The interaction term was significant for low and medium contrast but insignificant for targets with high contrast (H_0: β_3=0, α=.05, Bonferroni corrected for multiple comparisons across contrast levels). Because the interaction was significant for low and medium contrast, we turned to simple effect analysis and fitted a reduced model ($SRT \sim \beta_0 + \beta_1 * (targetEccentricity - 2)$) at each contrast level and for *Equal* and *Scaled* targets separately. For all *Equal* targets, SRT increased with increasing target eccentricity (H_0: β_1=0, α=.05, Bonferroni corrected for multiple comparisons across contrast levels and scaling groups). For the *Scaled* targets, the slope was significantly positive for medium and high contrast targets, but not significantly different from zero when the target contrast was low.

The above analysis suggests that foveal magnification modulates SRT in a similar fashion at different contrast levels but is most effective for low-contrast stimuli. One possibility is that the effect of scaling is itself scaled for different target contrast levels. When the target contrast is higher, SRT is generally shorter and thus leaves less room for scaling to reduce it further. Following this idea, to reveal the common mechanisms of scaling at different contrast levels, we normalized and combined data from different target contrast levels (Figure 3D, E). Similar to what was described in the previous section, we first fitted an exGauss for each SRT distribution plotted in Figure 3A and extracted the mode and FWHM to represent the typical value and variability of

the corresponding distribution. These values were then shifted and scaled as before such that for each target contrast level, the mode or FWHM spans zero to one. We next fitted a weighted linear regression model with interaction terms on these normalized modes or FWHMs ($Mode \sim \beta_0 + \beta_1 * (targetEccentricity - 2) + \beta_2 * (targetEccentricity - 2) * isScaled$ or $FWHM \sim \beta_0 + \beta_1 * (targetEccentricity - 2) + \beta_2 * (targetEccentricity - 2) * isScaled$). It turned out that for the mode, scaling significantly reduced the slope ($H_0: \beta_2$=0, α=.05). By contrast, the interaction term was not significant for FWHM. We next fitted a reduced model to analyze the simple effect of target eccentricity on Mode ($Mode \sim \beta_0 + \beta_1 * (targetEccentricity - 2)$) and the main effect on FWHM ($FWHM \sim \beta_0 + \beta_1 * (targetEccentricity - 2)$. The mode significantly increased with target eccentricity for *Equal* targets but not for *Scaled* targets ($Equal, CI_{\beta_1,95\%} = [.178, .257], Scaled, CI_{\beta_1,95\%} = [-.088, .134]$). FWHM significantly increased with target eccentricity ($Scaled, CI_{\beta_1,95\%} = [.164, .246]$) for *Scaled* and *Equal* targets combined.

Eccentricity-dependent SRT increment for endogenously driven saccade was not driven by foveal magnification but correlated with attentional orienting

So far, we focused on saccades in the *Step* task driven by the disappearance of the fixation point and the simultaneous appearance of a peripheral saccade target, which we refer to as exogenously driven saccades. In the following section, we switch to the *Overlap* task, in which response saccades were driven by the disappearance of the fixation point, while the peripheral saccade target had already been on for 800-1500 ms, such that we refer to them as endogenously driven saccades (Figure 1C). The same two stimulus sets, *Equal* and *Scaled* with full contrast filled white circles were used as target stimuli. Like the *Step* task, each trial in the *Overlap* task started with the monkey holding fixation on a fixation dot for 800 to 1000 ms. Then the target stimulus was presented for 800 to 1500 ms. Importantly during this period, the monkey was required to keep fixation on the fixation dot and restrain from making a saccade. Next, the fixation dot was turned off, which signaled the monkey to make a response saccade to the target stimulus. The monkey needed to shift its gaze to the target stimulus within 500 ms and hold its gaze on the target for another 800 to 1500 ms to complete the trial and receive a reward. Only correct trials were included in our analysis. Additionally, in 50% of the trials we included a short ≈30 ms flash at the fovea (1.0 dva diameter filled white circle) starting ≈100 ms after the fixation dot offset. The flash had no task relevance and was intended to capture attention back to the fovea when the response saccade was planned but, in most trials, not yet executed [18]. We collected data from three monkeys (KL, CH, HO) for this task.

We started with trials where no flash was presented (Figure 4). We started with testing whether scaling affected the medians of the SRT distributions. For monkeys KL and CH, this was true for targets at 8 and 10 dva (Mann-Whitney U test, α=.05, Bonferroni corrected for multiple comparisons across monkeys and target locations). Note that the direction of influence was opposite in KL and CH: scaling prolonged SRT for KL, but shortened SRT for CH. For monkey HO, scaling prolonged the SRT at all eccentricities, and this prolongation reached significance at all target eccentricities except 4 dva. Overall, in the *Overlap* task, the effect of scaling appeared small and variable across monkeys.

We next confirmed the varying influence of scaling in these three monkeys with linear regression (Figure 4B, $SRT \sim \beta_0 + \beta_1 * (targetEccentricity - 2) + \beta_2 * (targetEccentricity - 2) * IsScaled$). In line with results from Mann-Whitney U tests comparing individual SRT distributions, the

interaction term was significant for all monkeys but with different magnitudes and directions. In addition, the coefficients for scaling in the *Overlap* task had small magnitudes compared to the *Step* task (KL: 1.23 ms/dva (*Overlap*) vs. -3.6 ms/dva (*Step*); CH, -2.6 ms/dva vs. -4.5 ms/dva; HO, 3.28 ms/dva vs. -5.6 ms/dva). We continued by examining the simple effect of target location with a reduced model ($SRT \sim \beta_0 + \beta_1 * (targetEccentricity - 2)$). For monkey KL and CH, SRT increased with increasing target eccentricity both for *Equal* and *Scaled* targets (H_0: β_1=0, α=0.05, Bonferroni corrected for multiple comparisons across monkey and scaling groups). For monkey HO, the slope was not significant for *Scaled* targets and was significantly negative for *Equal* targets, but the effect size was very small, -1.2 ms/dva.

Next, we pooled the data across animals and fitted a weighted linear regression model for normalized exGauss mode and FWHM (Figure 4C-E, $Mode\ or\ FWHM \sim \beta_0 + \beta_1 * (targetEccentricity - 2) + \beta_2 * (targetEccentricity - 2) * isScaled$). For the mode, there was no significant difference between the *Scaled* and *Equal* targets. For FWHM, *Scaled* targets had a steeper slope. We next analyzed the simple effect of target eccentricity on the mode and FWHM: Both mode and FWHM increased with target eccentricity for both *Scaled* and *Equal* targets.

The observed increment of SRT with target eccentricity in the *Overlap* task is intriguing. Since the delay between target onset and fixation dot offset was at least 800 ms, the monkey had enough time to prepare for the impending saccade. The increment is therefore probably not related to motor planning before the "Go" signal. Rather, it is likely related to the processing that happened after the "Go" signal. Additionally, because the effect is eccentricity dependent, it is likely caused by spatially specific processing. One potential candidate is attentional orienting. Note that 1) because the "Go" signal is the fixation dot offset, to make a timely response, the animal needed to pay attention to the fovea, even though there were two stimuli (fixation dot and peripheral target) presented at the same time, 2) before actual saccade execution, attention is mandatorily shifted to the location of the saccade target [19]. Thus, the observed increment of SRT with target eccentricity can be explained if attentional orienting from the fovea takes longer for more eccentric targets.

An alternative explanation is that the eccentricity-dependent SRT increase is due to the fact that saccades were triggered by the removal of the fixation point. The fixation point is expected to exert an eccentricity-dependent inhibition on targets, such that its removal is expected to lead to an eccentricity-dependent release from inhibition [20-24]. To investigate this possibility, we presented a flash at the fovea, at ≈100 ms after fixation-point offset. This flash - in addition to dragging attention back to the fovea - is expected to add eccentricity-dependent inhibition, probably more than is released by the removal of the fixation point. If the addition of the flash is still followed by eccentricity-dependent SRTs, this would argue against an explanation based on eccentricity-dependent disinhibition. Figure 5A shows the SRT distributions in trials with foveal flash. To facilitate comparison, we plotted the exGauss fits obtained in corresponding conditions without flashes as dashed lines. As expected, the addition of the flash prolonged the SRT for all three monkeys [25, 26]. Importantly, the eccentricity-related SRT increase remained after the addition of the flash. We next quantified the observations with linear regression.

We started with an analysis for each monkey separately (Figure 5B). We first fitted an interaction model ($SRT \sim \beta_0 + \beta_1 * (targetEccentricity - 2) + \beta_2 * (targetEccentricity - 2) * IsScaled$). The interaction term was significant for CH and HO but with different signs (H_0: β_3=0; α=.05, Bonferroni corrected for multiple comparisons across monkeys). We next analyzed the simple

effect of target eccentricity ($sol \sim \beta_0 + \beta_1 * (targetEccentricity - 2)$). In all conditions, except *Equal* targets for HO, target eccentricity significantly increased SRT ($H_0: \beta_1$=0; α=.05, Bonferroni corrected for multiple comparisons across monkeys and conditions). With *Equal* targets in HO, target eccentricity did not show a significant effect on SRT.

Next, we combined data from the three monkeys by fitting a weighted linear regression model on normalized exGauss modes and FWHMs (Figure 5C-E). We started with an interaction model ($Mode\ or\ FWHM \sim \beta_0 + \beta_1 * (targetEccentricity - 2) + \beta_2 * (targetEccentricity - 2) * isScaled$). For both mode and FWHM, the interaction term was not significant ($H_0: \beta_3$=0; α=.05). We thus reduced the model to test for main effects ($Mode\ or\ FWHM \sim \beta_0 + \beta_1 * (targetEccentricity - 2)$. The modes of exGauss fits increased significantly with target eccentricity ($CI_{\beta_1,95\%} = [.073, .124]$). For FWHM, the slope did not reach significance, but showed a positive trend ($CI_{\beta_1,95\%} = [-.001, .077]$). This pattern of results is not consistent with predictions based on foveal disinhibition, yet it can be explained if attentional orienting from the fovea takes longer for more eccentric targets.

Discussion

Saccadic eye movements play a fundamental role in organizing our spatial and temporal visual input, to the extent that SRT has become a crucial psychophysical measurement enabling us to characterize the underlying cognitive processes that would otherwise remain unseen. However, despite the importance of this measurement, several fundamental questions regarding the determinants of SRT remain, even in relatively simple situations. In this study, we examined the dependence of SRT on target eccentricity in macaque monkeys. When designing the experiment, we based our hypotheses on previous insights into the role of the SC in generating the response saccades: Once the SC decision unit passes the response threshold, there is a relatively fixed delay in the downstream motor nuclei before the actual eye movement occurs [27, 28]. Consequently, any observed dependence of SRT on target eccentricity can be attributed to the spatiotemporal activation pattern of the SC, and reflects the properties of the neural mechanisms associated with that particular task. It is these properties that have clear behavioral correlates, namely SRT, the primary interest of the current study.

SRT in the *Step* task

In the *Step* task, afferent input to the SC was presumably dominated by the transient onset of the target stimulus. We first confirmed previous findings that, for medium-sized saccades, SRT increased with target eccentricity. Notably, this SRT increment was primarily explained by the foveal magnification factor (Figure 2, 3). A similar effect of foveal magnification neutralizing the eccentricity effect has been reported for a visual search task [29]. Furthermore, we showed that the foveal magnification factor interacted with stimulus contrast in determining the SRT. These observations align with the known properties of neurons in the SC. Specifically, the effect of foveal magnification can be explained by the Mexican-hat-like, short-distance excitatory, and long-distance inhibitory lateral interactions within the SC [24, 30, 31]. Because of this interaction pattern, given that we have chosen the targets to be overall small (< 0.13 mm in SC, according to Chen, et al. [8]), equal-sized targets located further away from the fovea should activate a smaller population of mutually facilitating neurons. As a result, the response threshold was expected to be crossed more slowly, leading to longer SRTs. When we scaled the stimulus size according to the SC magnification factor, the lateral interaction pattern would predict an equal

SRT at all eccentricities, which is what we found for the *Scaled* targets. The observation that foveal magnification modulated SRT most effectively for low-contrast stimuli can be explained by the fact that higher contrast or higher luminance stimuli evoke larger responses in the SC [17, 32]. If this drives activation already close to the threshold, the effect of facilitation by nearby neurons is expected to be small. Together, these findings imply a direct translation of stimulus salience to response urgency mediated by the SC [33]. Future studies employing a neural field model can help describe such interactions quantitatively [30, 34, 35].

SRT in the *Overlap* task

In the *Overlap* task, when the monkey was about to make the response saccade, the target had already been on the screen for at least 800 ms, long beyond the target-onset-related visual burst in the SC neurons, which diminishes around 100 ms after the stimulus onset [36, 37]. As a result, afferent input relevant to the response saccade was no longer expected to be dominated by the transient onset of the target stimulus. In agreement with this prediction, in the *Overlap* task, the dependence of SRT on eccentricity was no longer affected by scaling. Yet, the simple dependence of SRT on eccentricity was still present, leading to the question: What is the mechanism underlying this SRT increment? One potential candidate is attentional orienting. Results from trials with flashes provided further evidence supporting this hypothesis, as explained in the Result. If the observed SRT increment was indeed related to attentional orienting, the regression slopes inform us about how fast attention was moving from the fovea to the peripheral targets: ≈3.2 to 3.6 ms/dva in the three monkeys. This value is in a similar range as the speed of covert attentional scanning estimated in a recent paper [38].

Variability of SRT

As noted in previous studies, SRT exhibited significant trial-by-trail variation in both the *Step* and *Overlap* tasks. Within the framework of a rise-to-threshold model, a larger variance in SRT means either a higher threshold or a more variable rate of rise [5, 12, 13, 30]. A consistent finding in our study is the increased variability of SRT for targets located in the periphery. This pattern held true for both *Equal* and *Scaled* targets in both the *Step* and *Overlap* tasks. Notably, in the *Step* task with *Scaled* targets, SRT variance increased with target eccentricity, despite the effective flattening of the SRT mode by scaling (Figure 2, 3). These findings suggest that factors beyond foveal magnification, and to some degree invariant to the task, contributed to the observed SRT variance increment with target eccentricity. One potential mechanism could be that neuronal response fields (both motor and visual) of larger eccentricity typically have larger size. Larger response field sizes likely lead to less specific, or in other words, noisier contributions to the ensuing saccade. When cortical magnification is controlled, this leads to higher noise in the recruited neuronal population. Interestingly, Hafed and Chen [39] reported a weaker and more variable visual response associated with less accurate saccades in SC neurons with a larger response field. Note that these authors compared neurons representing lower versus upper visual fields, yet similar properties are conceivable comparing neurons with response fields centered at different eccentricities.

Individual differences

We observed considerable variations in SRT distributions among the four monkeys tested. These variations likely have multiple sources. Firstly, variations associated with scaling can be partially explained by the individual differences in foveal magnification factors [40]. Secondly, some undue

variance in reaction time distributions could be related to the task design. Most prominently, the maximum reaction time allowed was 500 ms at all locations in all tasks. This setting is essential for assuring the same task structure across all conditions, but it is not optimal for eliminating the influence of task-irrelevant processes. Indeed, the monkeys whose SRTs showed the largest variance, suggesting extra noise in their decision process, were also the ones that seemed to be the outliers (HU in Figure 2 and HO in Figure 4). Since using a large response window is required to compare SRT distributions that are expected to shift significantly, future studies can use variable reward amounts to encourage the animal to make as fast a response as possible and potentially reduce the variability among the subjects [41].

Increasing the number of subjects is crucial for obtaining a more comprehensive understanding of whether the observed effect is present in the population. However, in the current study, the number of subjects was limited, partly because of the chosen animal model, i.e. macaques. Macaque monkeys were used due to the availability of published data on the foveal magnification factor in the SC, which was essential for the experimental design. In human studies, it is generally easier to include a larger number of subjects; however, the lack of foveal magnification factor data in humans poses a challenge. Nevertheless, it is not unreasonable to utilize the same magnification factor as observed in macaque monkeys. Alternatively, one can consider using the magnification factor measured for the primary visual cortex, as evidence indicates that the magnification factor of primary visual cortex and SC are similar [8].

Author contribution

YZ: Conceptualization, Methodology, Software, Validation, Formal Analysis, Investigation, Data Curation, Writing – Original Draft; Writing-Reviewing & Editing; PF: Methodology, Validation, Resources, Writing – Original Draft, Writing-Reviewing & Editing, Supervision, Funding Acquisition.

Declaration of interests

P.F. is member of the Advisory Board of CorTec GmbH (Freiburg, Germany). The authors declare no further competing interests.

Acknowledgement

The authors would like to thank Ziad Hafed for helpful discussions about the study, Tim Näher for advice on data analysis, Jackson Smith for training of monkey HO, and Sabrina Wallrath, Julia Hoffmann and Marianne Hartmann for technical support with monkey training and behavioral data collection.

Figure legends

Figure 1. Stimuli and task. **(A)** Representation of target stimuli on the screen and their corresponding representation in the SC, based on the foveal magnification reported in Chen, et al. [8]. Top: *Equal* targets at varying eccentricities on the screen exhibit a diminishing size of corresponding neuronal representations in the SC. Bottom: *Scaled* targets on the screen have the same size of corresponding neuronal representations in the SC. **(B)** In the *Step task*, the fixation dot stepped into the periphery and became the target stimulus. **(C)** In the *Overlap* task, the target presentation preceded the fixation dot removal. The animal was required to wait until the removal of the fixation dot before shifting its gaze. In 50% of trials, a transient foveal flash was presented at ≈100 ms after fixation dot removal. The flash had no task relevance and served to capture attention back to the fovea while the response saccade was planned but not yet executed.

Figure 2. Eccentricity-dependent SRT in the *Step* task. **(A)** Distribution of SRT for targets at different eccentricities, plotted separately for *Equal* (blue) and *Scaled* (orange) targets. Solid lines represent the fitted exponentially modified Gaussian (exGauss) distributions. The dashed lines indicate the modes of the fit, and the shaded regions show the 95% bootstrap confidence intervals. **(B)** Robust linear regression of raw SRT on target eccentricity. For better visibility, the raw SRT values were horizontally jittered around the corresponding target locations. **(C)** Weighted linear regression of normalized exGauss fit mode on target eccentricity. **(D)** Same as (C) but for the normalized exGauss fit full width at half maximum (FWHM). **(E)** Regression table for the analyses in (C) and (D) along with the results of the simple effect analyses.

Figure 3. Eccentricity-dependent SRT for targets of different contrast. **(A)** Distribution of SRTs for targets of low, medium and high contrast, grouped by target eccentricity, plotted separately for *Equal* (blue) and *Scaled* (orange) targets. Solid lines represent the fitted exGauss distributions. The dashed lines indicate the mode of the fit, and the shaded regions show the 95% bootstrap confidence intervals. **(B)** Robust linear regression of raw SRTs on target log contrast, defined as $\log(\frac{I_{tar}-I_b}{I_b})$. For better visibility, the raw SRT values were jittered horizontally around the corresponding contrast levels. **(C)** Same as (B) but on target eccentricity. **(D)** Weighted linear regression of normalized exGauss fit mode on target eccentricity. **(E)** Same as (D) but for the normalized exGauss fit full width at half maximum (FWHM). **(F)** Regression table for the analyses in (D) and (E) along with the results of the simple-effect analyses.

Figure 4. Eccentricity-dependent SRT in the *Overlap* task without foveal flash. **(A)** Distribution of SRTs for targets at different eccentricities, plotted separately for *Equal* (blue) and *Scaled* (orange) targets. Solid lines represent the fitted exponentially modified Gaussian (exGauss) distribution. The dashed lines indicate the modes of the fits, and the shaded regions show the 95% bootstrap confidence intervals. **(B)** Robust linear regression of raw SRTs on target eccentricity. For better visibility, the raw SRT values were horizontally jittered around the corresponding target locations. **(C)** Weighted linear regression of normalized exGauss fit mode on target eccentricity. **(D)** Same as (C) but for the normalized exGauss fit full width at half maximum (FWHM). **(E)** Regression table for the analyses in (C) and (D) along with the results of the simple effect analyses.

Figure 5. Eccentricity-dependent SRT in the *Overlap* task with foveal flash. **(A)** Distribution of SRTs for targets at different eccentricities, plotted separately for *Equal* (blue) and *Scaled* (orange) targets. Solid lines represent the fitted exponentially modified Gaussian (exGauss) distribution.

ExGauss distributions shown as dashed lines represent the SRT distributions in corresponding conditions without the foveal flash (as in Figure 4). Vertical dashed lines indicate the mode of the fit, and the shaded regions show the 95% bootstrap confidence intervals. **(B)** Robust linear regression of raw SRTs on target eccentricity. For better visibility, the raw SRT values were horizontally jittered around the corresponding target locations **(C)** Weighted linear regression of normalized exGauss fit mode on target eccentricity. **(D)** Same as (C) but for the normalized exGauss fit full width at half maximum (FWHM). **(E)** Regression table for the analyses in (C) and (D) along with the results of the simple-effect and main-effect analyses.

STAR Methods

Subjects

Four male adult monkeys (Macaca mulatta) participated in the current study (referred to as CH, HO, KL and HU). All experimental procedures were conducted in compliance with the German and European animal protection laws. The experiments were approved by the responsible local authority, the Regierungspräsidium Darmstadt. All animals were implanted with a titanium headpost [42]. Additionally, Monkey KL and HO had recording chambers implanted for addressing other scientific questions. The animals' water intake was regulated to ensure their motivation during the behavioral task in which a small juice reward was provided after each correct trial.

Visual stimuli

All stimuli were controlled by custom software (https://github.com/esi-neuroscience/ARCADE), and presented on an LCD monitor (LG 32GK850G-B) at 143.9Hz. Viewing distance was 78 cm for all monkeys. Precise stimulus presentation time was validated with a photodiode attached to the screen. Parameters for all stimuli used are listed below.

Fixation dot. Trials in all tasks started with presenting a fixation dot. The fixation dot in all trials was a white filled cycle of 0.1 dva diameter, 243.7cd/m^2, at the center of the screen.

Target stimuli. Each trial contained a single target stimulus, which was chosen randomly from a set specified by the task. Specifically, the stimulus set in the *Step* task contained targets centered at 2, 3, 4, 5, 6, 8, and 10 dva, along the horizontal median to the right of the screen. At each target location, the set contained one target belonging to the *Equal* group and one target belonging to the *Scaled* group. For the *Equal* group, the target was a white filled circle of 0.1 dva, 243.7 cd/ m^2 at all eccentricities. For the *Scaled* group, the target was a white filled circle of 243.7 cd/ m^2 and 0.1, 0.13, 0.17, 0.20, 0.24, 0.31, 0.38 dva diameters at 2, 3, 4, 5, 6, 8, and 10 dva, respectively. In the modified *Step* task with variable target contrast, the target locations were limited to 2, 4, and 6 dva, and at each eccentricity and for both *Scaled* and *Equal* targets, the possible target set contained targets of three different luminance levels: namely low contrast, 74.57 cd/ m^2; medium contrast, 124.66 cd/ m^2 and high contrast 243.7 cd/ m^2.

Screen background. Gray background was used in all tasks. Except for the modified *Step* task with variable target contrast, the screen background luminance was 60.0 cd/ m^2. In the modified *Step* task, the screen background luminance was 30.7 cd/ m^2.

Foveal flash. The foveal flash used in the *Overlap* task was a white filled circle of 1.0 dva and 243.7 cd/ m^2.

Behavioral tasks

We recorded the binocular gaze data at 500 Hz with an Eyelink-1000 system (SR Research Ltd.). Real-time gaze data from one eye was used for online behavioral control.

Step task (Figure 1B). In the *Step* task, after fixation was acquired and maintained for 800 to 1500 ms, the fixation dot was removed, and in the same video frame, a single target was presented in the periphery. The animal needed to make a saccade, within 500 ms, to the target and hold its gaze on the target for another 800 to 1500 ms to obtain the juice reward.

Overlap task (Figure 1C). In the *Overlap* task, after the fixation was acquired and maintained for 800 to 1000 ms, without removal of the fixation point, a single target was presented in the periphery for 800 to 1500 ms after which the fixation dot was removed. Only after fixation dot removal, the monkey was allowed to make a saccade to the target, and it needed to make a saccade towards the target within 500 ms and hold its gaze on the target for another 800 to 1500 ms to successfully complete the trial and obtain the reward. Additionally, in 50% of the trials in the *Overlap* task, we included a ≈30 ms flash at the fovea (white-filled circle of 1.0 dva diameter) presented ≈100 ms after the fixation dot offset. The flash had no task relevance, and the monkey needed to complete the trial as in trials without flash.

Trial inclusion

Only correct trials were included in the analysis. Additionally: 1) Trials with SRTs less than 100 ms were excluded from all tasks. 2) In *Overlap*-task trials containing a foveal flash, any trial with the response saccade occurring within 100 ms after the flash was also excluded.

Saccade detection and SRT definition

Saccades were detected using a two-dimensional velocity threshold, following the methodology described in Engbert and Kliegl [43]. In our analysis, we set lambda to 10. Saccade onset time was determined as the moment when the velocity threshold was crossed. In all tasks, SRT was defined as the time elapsed between the offset of the fixation dot and the onset of the response saccade.

Regression analysis

The regression analysis was performed with the Python module statsmodels [44]. Further details can be found in the corresponding Results section.

References

1. Hafed, Z.M., and Goffart, L. (2020). Gaze direction as equilibrium: more evidence from spatial and temporal aspects of small-saccade triggering in the rhesus macaque monkey. Journal of neurophysiology *123*, 308-322.

2. Kalesnykas, R.P., and Hallett, P.E. (1994). Retinal eccentricity and the latency of eye saccades. Vision research *34*, 517-531.

3. Land, M., Mennie, N., and Rusted, J. (1999). The roles of vision and eye movements in the control of activities of daily living. Perception *28*, 1311-1328.

4. Rohenkohl, G., Bosman, C.A., and Fries, P. (2018). Gamma Synchronization between V1 and V4 Improves Behavioral Performance. Neuron *100*, 953-963 e953.

5. Hanes, D.P., and Schall, J.D. (1996). Neural control of voluntary movement initiation. Science *274*, 427-430.

6. Liversedge, S.P., Gilchrist, I.D., and Everling, S. (2011). The Oxford handbook of eye movements, (Oxford ; New York: Oxford University Press).

7. Ottes, F.P., Van Gisbergen, J.A., and Eggermont, J.J. (1986). Visuomotor fields of the superior colliculus: a quantitative model. Vision research *26*, 857-873.

8. Chen, C.Y., Hoffmann, K.P., Distler, C., and Hafed, Z.M. (2019). The Foveal Visual Representation of the Primate Superior Colliculus. Current biology : CB *29*, 2109-2119 e2107.

9. Azzopardi, P., and Cowey, A. (1996). The overrepresentation of the fovea and adjacent retina in the striate cortex and dorsal lateral geniculate nucleus of the macaque monkey. Neuroscience *72*, 627-639.

10. Findlay, J.M. (1980). The visual stimulus for saccadic eye movements in human observers. Perception *9*, 7-21.

11. Doma, H., and Hallett, P.E. (1988). Rod-cone dependence of saccadic eye-movement latency in a foveating task. Vision research *28*, 899-913.

12. Carpenter, R.H., and Williams, M.L. (1995). Neural computation of log likelihood in control of saccadic eye movements. Nature *377*, 59-62.

13. Ratcliff, R., and McKoon, G. (2008). The diffusion decision model: theory and data for two-choice decision tasks. Neural computation *20*, 873-922.

14. Lee, J., Williford, T., and Maunsell, J.H. (2007). Spatial attention and the latency of neuronal responses in macaque area V4. The Journal of neuroscience : the official journal of the Society for Neuroscience *27*, 9632-9637.

15. Gawne, T.J., Kjaer, T.W., and Richmond, B.J. (1996). Latency: another potential code for feature binding in striate cortex. Journal of neurophysiology *76*, 1356-1360.

549 16. Tanaka, T., Nishida, S., Aso, T., and Ogawa, T. (2013). Visual response of neurons in
550 the lateral intraparietal area and saccadic reaction time during a visual detection task. The
551 European journal of neuroscience *37*, 942-956.

552 17. Bell, A.H., Meredith, M.A., Van Opstal, A.J., and Munoz, D.P. (2006). Stimulus intensity
553 modifies saccadic reaction time and visual response latency in the superior colliculus.
554 Experimental brain research *174*, 53-59.

555 18. Nakayama, K., and Mackeben, M. (1989). Sustained and transient components of focal
556 visual attention. Vision research *29*, 1631-1647.

557 19. Deubel, H., and Schneider, W.X. (1996). Saccade target selection and object
558 recognition: evidence for a common attentional mechanism. Vision research *36*, 1827-1837.

559 20. Dorris, M.C., Paré, M., and Munoz, D.P. (1997). Neuronal activity in monkey superior
560 colliculus related to the initiation of saccadic eye movements. The Journal of neuroscience : the
561 official journal of the Society for Neuroscience *17*, 8566-8579.

562 21. Munoz, D.P., and Istvan, P.J. (1998). Lateral inhibitory interactions in the intermediate
563 layers of the monkey superior colliculus. Journal of neurophysiology *79*, 1193-1209.

564 22. Meredith, M.A., and Ramoa, A.S. (1998). Intrinsic circuitry of the superior colliculus:
565 pharmacophysiological identification of horizontally oriented inhibitory interneurons. Journal of
566 neurophysiology *79*, 1597-1602.

567 23. Phongphanphanee, P., Marino, R.A., Kaneda, K., Yanagawa, Y., Munoz, D.P., and Isa,
568 T. (2014). Distinct local circuit properties of the superficial and intermediate layers of the rodent
569 superior colliculus. The European journal of neuroscience *40*, 2329-2343.

570 24. Munoz, D.P., and Fecteau, J.H. (2002). Vying for dominance: dynamic interactions
571 control visual fixation and saccadic initiation in the superior colliculus. Progress in brain
572 research *140*, 3-19.

573 25. Buonocore, A., and McIntosh, R.D. (2008). Saccadic inhibition underlies the remote
574 distractor effect. Experimental brain research *191*, 117-122.

575 26. Reingold, E.M., and Stampe, D.M. (2002). Saccadic inhibition in voluntary and reflexive
576 saccades. Journal of cognitive neuroscience *14*, 371-388.

577 27. Schall, J.D., and Paré, M. (2021). The unknown but knowable relationship between
578 Presaccadic Accumulation of activity and Saccade initiation. Journal of computational
579 neuroscience *49*, 213-228.

580 28. Gandhi, N.J., and Katnani, H.A. (2011). Motor functions of the superior colliculus. Annual
581 review of neuroscience *34*, 205-231.

582 29. Carrasco, M., and Frieder, K.S. (1997). Cortical magnification neutralizes the eccentricity
583 effect in visual search. Vision research *37*, 63-82.

30. Trappenberg, T.P., Dorris, M.C., Munoz, D.P., and Klein, R.M. (2001). A model of saccade initiation based on the competitive integration of exogenous and endogenous signals in the superior colliculus. Journal of cognitive neuroscience *13*, 256-271.

31. Isa, T., Marquez-Legorreta, E., Grillner, S., and Scott, E.K. (2021). The tectum/superior colliculus as the vertebrate solution for spatial sensory integration and action. Current biology : CB *31*, R741-R762.

32. Chen, C.Y., and Hafed, Z.M. (2018). Orientation and Contrast Tuning Properties and Temporal Flicker Fusion Characteristics of Primate Superior Colliculus Neurons. Frontiers in neural circuits *12*, 58.

33. Veale, R., Hafed, Z.M., and Yoshida, M. (2017). How is visual salience computed in the brain? Insights from behaviour, neurobiology and modelling. Philosophical transactions of the Royal Society of London. Series B, Biological sciences *372*.

34. Taouali, W., Goffart, L., Alexandre, F., and Rougier, N.P. (2015). A parsimonious computational model of visual target position encoding in the superior colliculus. Biological cybernetics *109*, 549-559.

35. Marino, R.A., Levy, R., Boehnke, S., White, B.J., Itti, L., and Munoz, D.P. (2012). Linking visual response properties in the superior colliculus to saccade behavior. The European journal of neuroscience *35*, 1738-1752.

36. Hafed, Z.M., Hoffmann, K.P., Chen, C.Y., and Bogadhi, A.R. (2023). Visual Functions of the Primate Superior Colliculus. Annual review of vision science.

37. Goldberg, M.E., and Wurtz, R.H. (1972). Activity of superior colliculus in behaving monkey. I. Visual receptive fields of single neurons. Journal of neurophysiology *35*, 542-559.

38. Fries, P. (2023). Rhythmic attentional scanning. Neuron *111*, 954-970.

39. Hafed, Z.M., and Chen, C.Y. (2016). Sharper, Stronger, Faster Upper Visual Field Representation in Primate Superior Colliculus. Current biology : CB *26*, 1647-1658.

40. Van Essen, D.C., Newsome, W.T., and Maunsell, J.H. (1984). The visual field representation in striate cortex of the macaque monkey: asymmetries, anisotropies, and individual variability. Vision research *24*, 429-448.

41. Fischer, B., and Wegener, D. (2018). Emphasizing the "positive" in positive reinforcement: using nonbinary rewarding for training monkeys on cognitive tasks. Journal of neurophysiology *120*, 115-128.

42. Psarou, E., Vezoli, J., Schölvinck, M.L., Ferracci, P.-A., Zhang, Y., Grothe, I., Roese, R., and Fries, P. (2022). Modular, cement-free, customized headpost and connector-chamber implants for macaques. bioRxiv, 2022.2011.2009.515849.

43. Engbert, R., and Kliegl, R. (2003). Microsaccades uncover the orientation of covert attention. Vision research *43*, 1035-1045.

44. Seabold, Skipper, and Perktold, J. (2010). statsmodels: Econometric and statistical modeling with python.

Figure 1

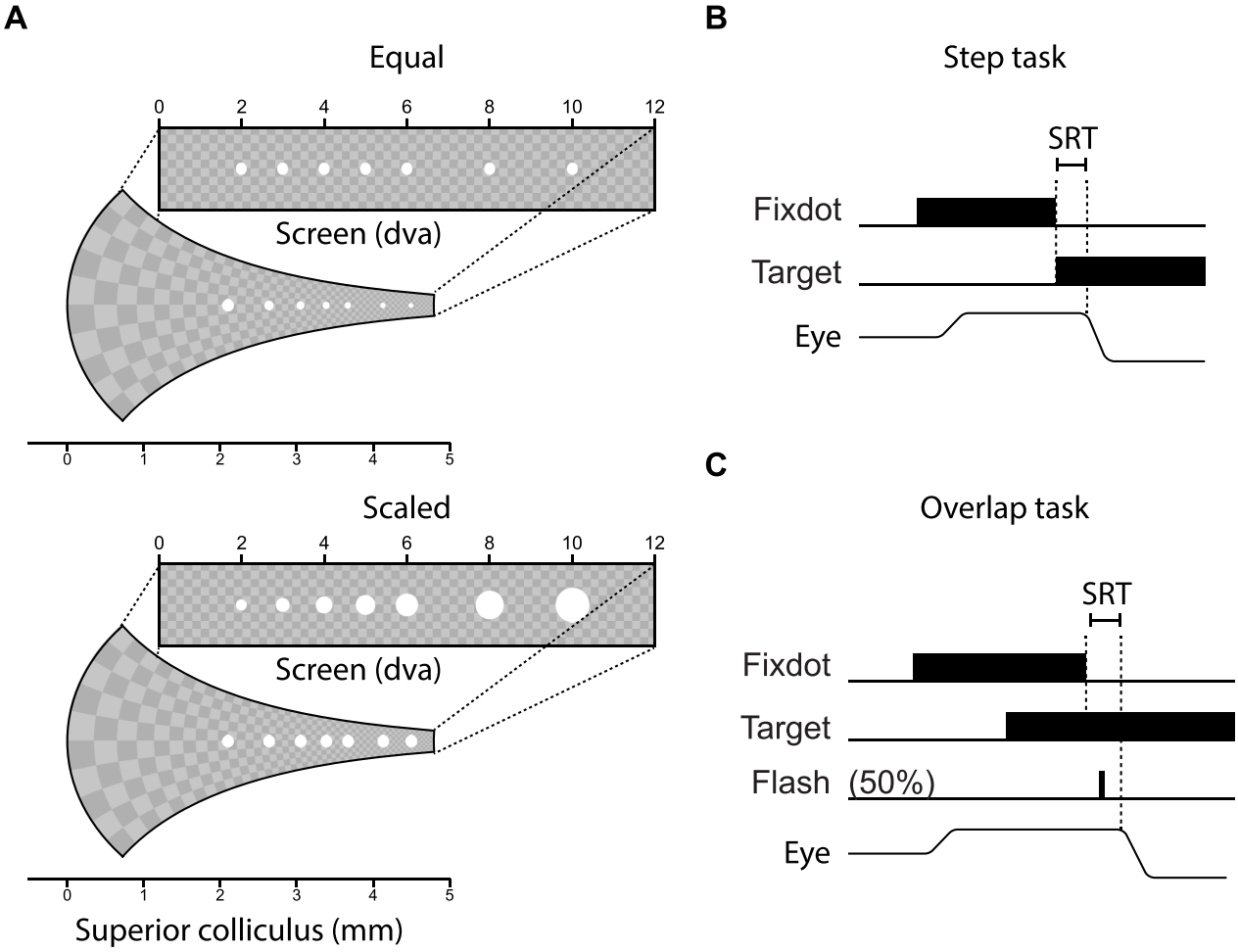
A
Equal
0
2
4
6
8
10
12
Screen (dva)
0
1
2
3
4
5
Scaled
0
2
4
6
8
10
12
Screen (dva)
0
1
2
3
4
5
Superior colliculus (mm)
B
Step task
SRT
Fixdot
Target
Eye
C
Overlap task
SRT
Fixdot
Target
Flash
(50%)
Eye

Figure 2

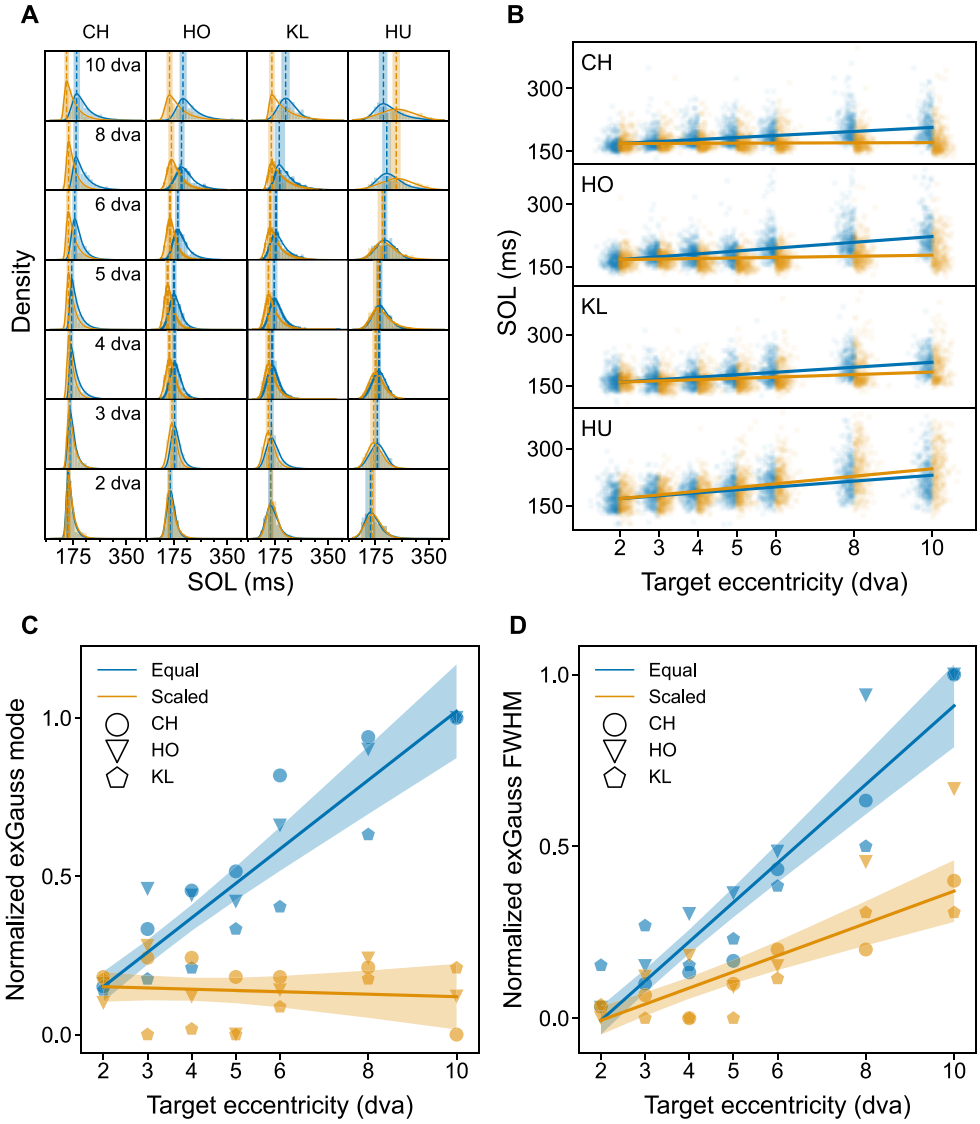

E

Mode		coef	std err	t	P > |t|	[0.025	0.975]
Equal	Intercept	0.1530	0.037	4.087	0.001	0.075	0.231
$R^2 = 0.776$	tarEcc-2	0.1082	0.013	8.105	0.000	0.080	0.136
Scaled	Intercept	0.1498	0.030	4.960	0.000	0.087	0.213
$R^2 = 0.009$	tarEcc-2	-0.0036	0.009	-0.415	0.683	-0.022	0.015
Combined (full)	Intercept	0.1512	0.023	6.465	0.000	0.104	0.198
$R^2 = 0.767$	tarEcc-2	0.1087	0.011	10.310	0.000	0.087	0.130
	isScaled*(tarEcc-2)	-0.1127	0.011	-10.709	0.000	-0.134	-0.091

FWHM		coef	std err	t	P > |t|	[0.025	0.975]
Equal	Intercept	0.0083	0.033	0.254	0.802	-0.060	0.076
$R^2 = 0.843$	tarEcc-2	0.1107	0.011	10.113	0.000	0.088	0.134
Scaled	Intercept	-0.0173	0.026	-0.652	0.522	-0.073	0.038
$R^2 = 0.683$	tarEcc-2	0.0495	0.008	6.393	0.000	0.033	0.066
Combined (full)	Intercept	-0.0063	0.020	-0.306	0.761	-0.048	0.035
$R^2 = 0.819$	tarEcc-2	0.1144	0.009	13.185	0.000	0.097	0.132
	isScaled*(tarEcc-2)	-0.0674	0.009	-7.743	0.000	-0.085	-0.050

Figure 3

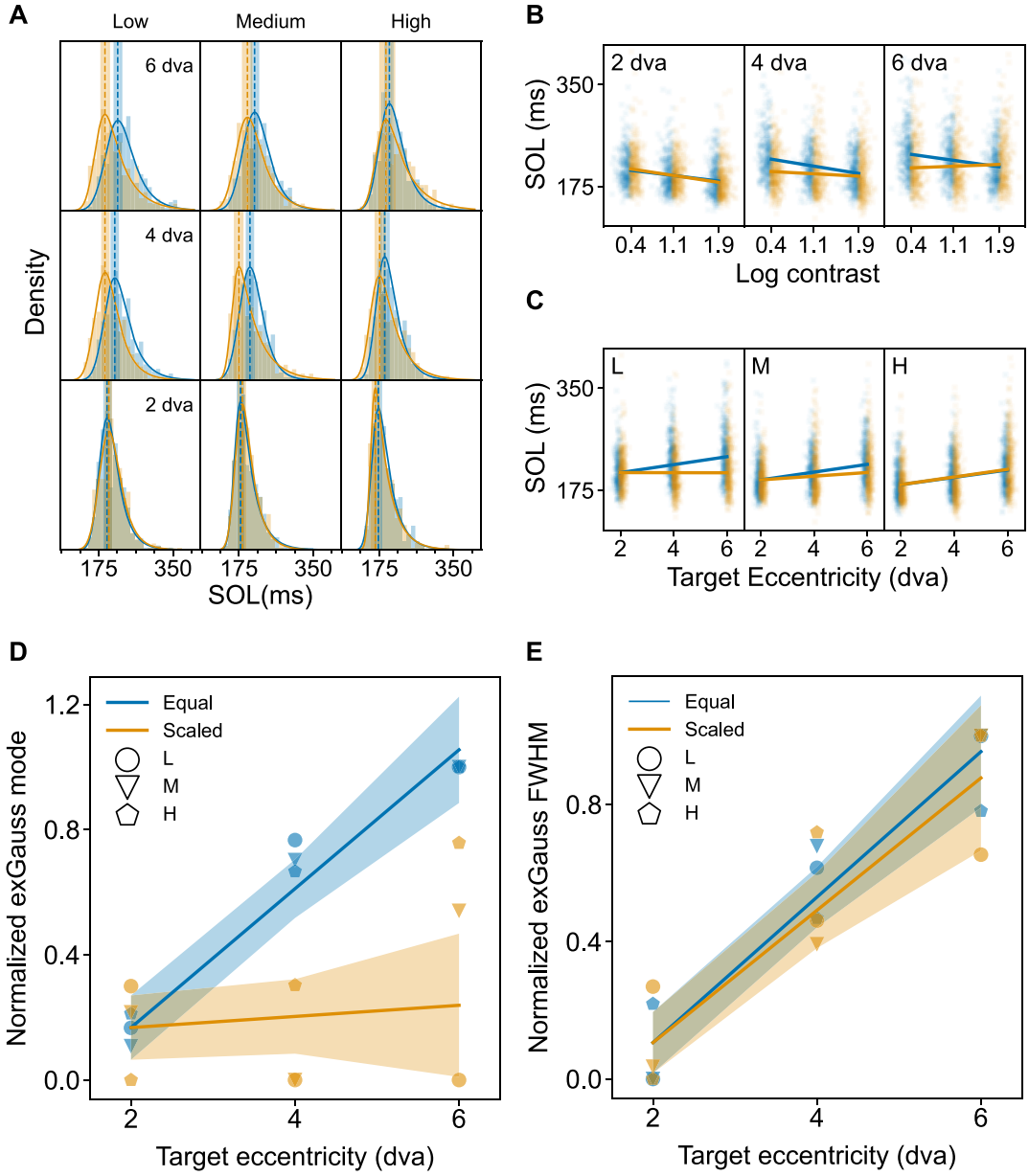

F

		Mode					
		coef	std err	t	P > |t|	[0.025	0.975]
Equal	Intercept	0.1812	0.039	4.652	0.002	0.089	0.273
$R^2 = 0.961$	tarEcc-2	0.2178	0.017	13.084	0.000	0.178	0.257
Scaled	Intercept	0.1512	0.095	1.589	0.156	-0.074	0.376
$R^2 = 0.033$	tarEcc-2	0.0231	0.047	0.491	0.638	-0.088	0.134
Combined (full)	Intercept	0.1675	0.048	3.474	0.003	0.065	0.270
$R^2 = 0.853$	tarEcc-2	0.2219	0.025	9.039	0.000	0.170	0.274
	isScaled*(tarEcc-2)	-0.2041	0.033	-6.156	0.000	-0.275	-0.133
		FWHM					
		coef	std err	t	P > |t|	[0.025	0.975]
Combined (main)	Intercept	0.1054	0.041	2.569	0.021	0.018	0.192
$R^2 = 0.877$	tarEcc-2	0.2051	0.019	10.546	0.000	0.164	0.246

Figure 4

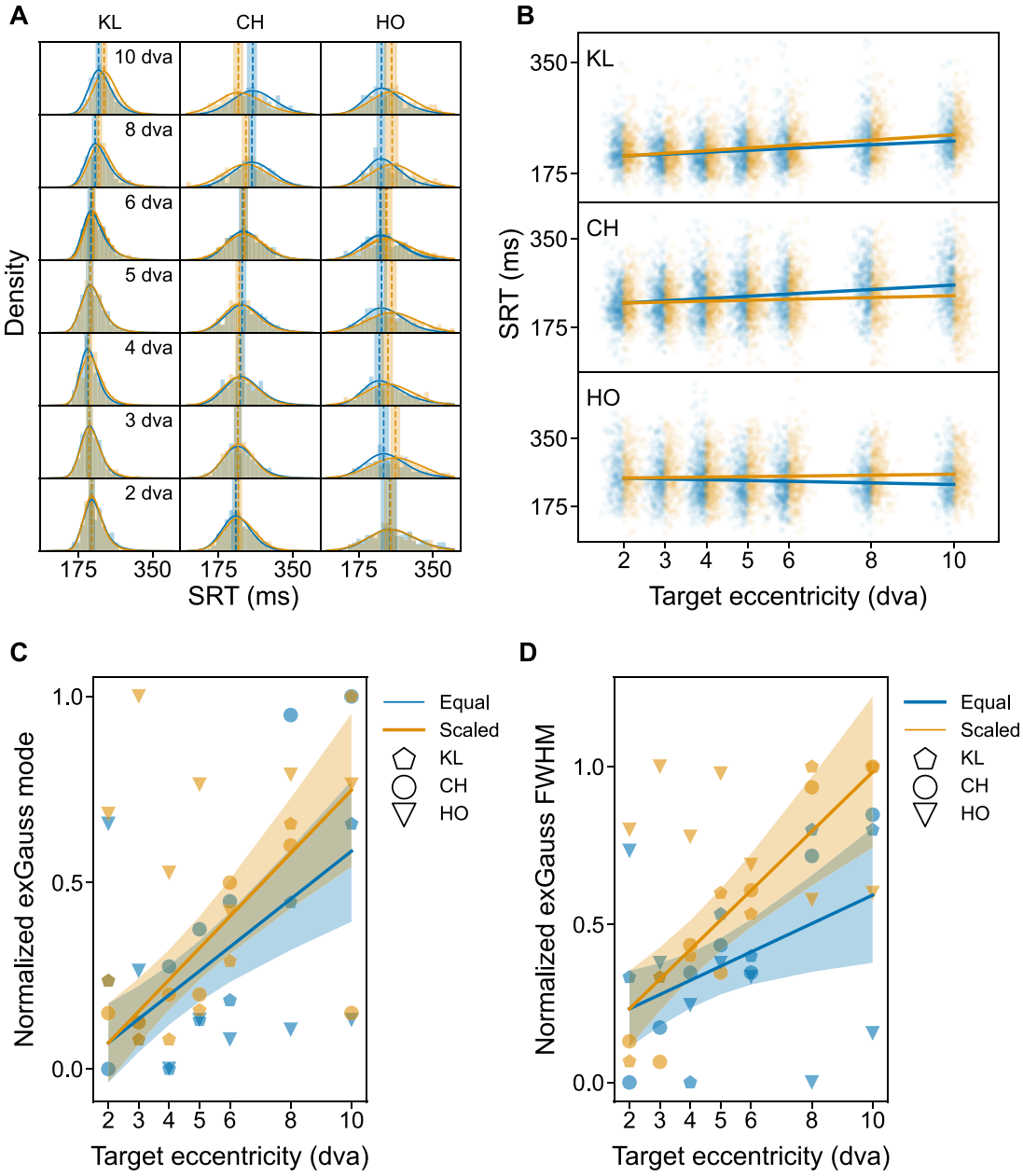

E

		Mode					
		coef	std err	t	P > |t|	[0.025	0.975]
Combined (main)	Intercept	0.0718	0.053	1.361	0.181	-0.035	0.179
$R^2 = 0.459$	tarEcc-2	0.0734	0.013	5.576	0.000	0.047	0.100
		FWHM					
		coef	std err	t	P > |t|	[0.025	0.975]
Equal	Intercept	0.1965	0.078	2.535	0.020	0.034	0.359
$R^2 = 0.277$	tarEcc-2	0.0524	0.019	2.698	0.014	0.012	0.093
Scaled	Intercept	0.2725	0.093	2.937	0.008	0.078	0.467
$R^2 = 0.401$	tarEcc-2	0.0858	0.024	3.563	0.002	0.035	0.136
Combined (full)	Intercept	0.2332	0.060	3.900	0.000	0.112	0.354
$R^2 = 0.397$	tarEcc-2	0.0450	0.017	2.604	0.013	0.010	0.080
	isScaled*(tarEcc-2)	0.0487	0.019	2.593	0.013	0.011	0.087

Figure 5

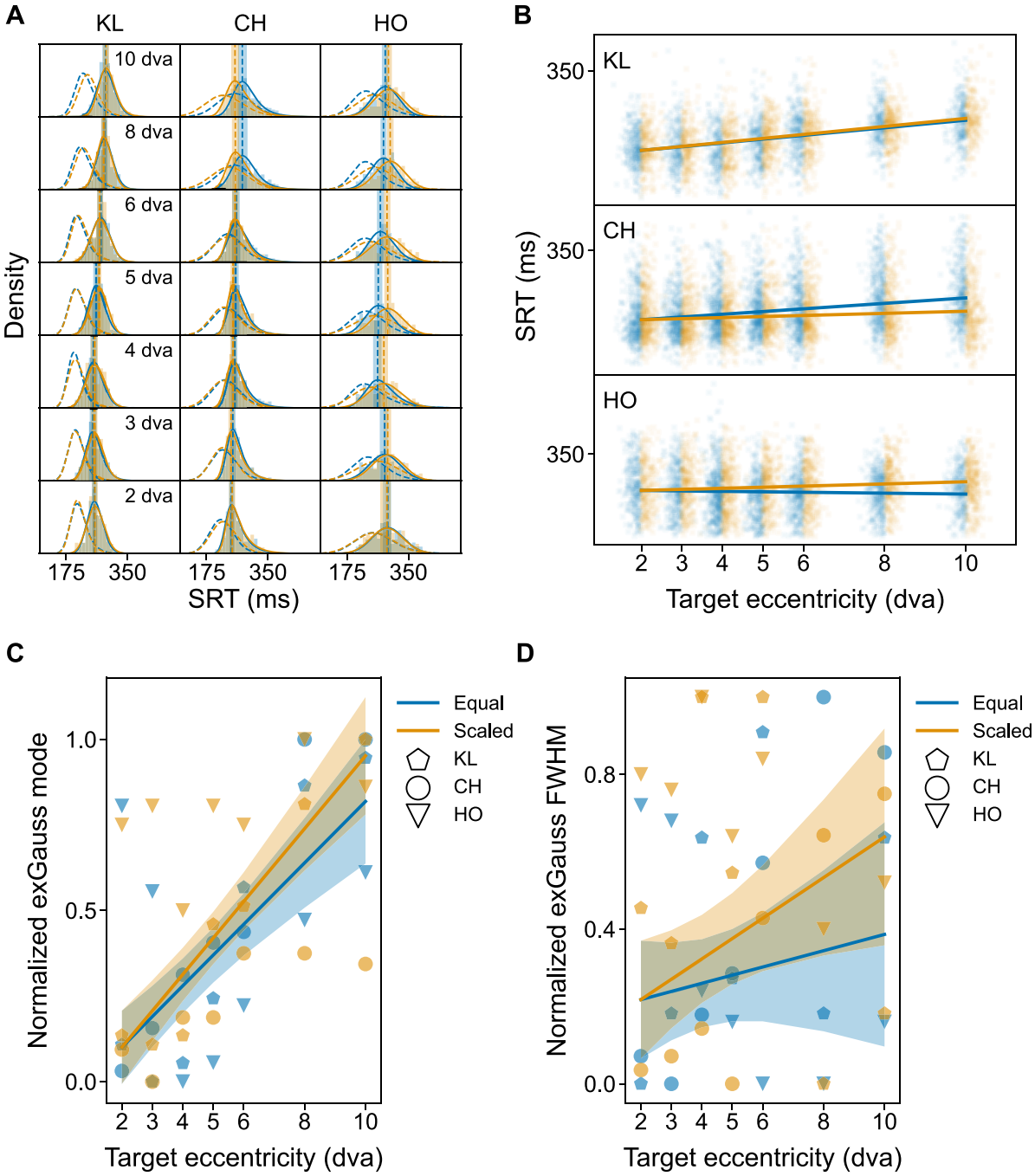

E

Mode		coef	std err	t	P > |t|	[0.025	0.975]
Combined(main)	Intercept	0.1013	0.053	1.911	0.063	-0.006	0.209
$R^2 = 0.613$	tarEcc-2	0.0985	0.012	7.952	0.000	0.073	0.124

FWHM		coef	std err	t	P > |t|	[0.025	0.975]
Combined(main)	Intercept	0.2163	0.076	2.845	0.007	0.063	0.370
$R^2 = 0.087$	tarEcc-2	0.0376	0.019	1.950	0.058	-0.001	0.077